PulseChord

Hariz Zoran Farooq[1,*]

[1]Independent Designer [*]Corresponding author:
harizzoranfarooq@gmail.com

***Abstract*—PulseChord is a purely analog haptic feedback belt that converts live audio into tactile vibrations through voice coil actuators positioned around the torso/waist. Designed to create an immersive sensory experience, it delivers real-time feedback corresponding to musical rhythm and dynamics. Unlike digital solutions, PulseChord requires no microcontrollers or signal processors, resulting in lower latency, reduced power consumption, and simplified design. In particular, it offers a low-cost, intuitive alternative for individuals who are deaf or hard of hearing, enabling access to audio cues through vibration. This makes it especially promising as a tool for experiencing music non-audibly, translating musical content into physically perceptible sensations. Additional applications include musical performances, interactive media, and other scenarios where non-visual, real-time feedback is valuable. A complete proof-of-concept prototype has been fabricated and tested, demonstrating stable analog operation and effective signal band separation.**

I. Introduction

This paper presents the design and application of *PulseChord*, a purely analog haptic feedback belt developed by the author. The system employs third-order Sallen–Key active filters to split live audio into three frequency bands optimized for skin sensitivity. These filtered signals are then mapped to voice coil actuators distributed throughout the torso/waist, providing real-time tactile feedback without requiring digital signal processing. PulseChord thus offers an accessible and low-cost alternative to existing haptic technologies, with potential applications including assistive tools for the deaf and hard of hearing, immersive musical experiences, and enhanced sensory feedback in gaming and virtual reality. Human tactile perception is mediated by mechanoreceptors such as Meissner and Pacinian corpuscles, which are sensitive to different frequency ranges. Meissner corpuscles respond most strongly around 60 Hz, while Pacinian corpuscles are sensitive from 20 Hz to 800 Hz, peaking near 250 Hz [1]. Studies have reported that the overall tactile sensitivity spans from approximately 0.4 to 1000 Hz, with optimal perception near 250 Hz. Vibrations primarily stimulate Pacinian and Meissner's corpuscles, with low frequencies (< 60 Hz) sensed by non-Pacinian pathways and high frequencies (> 60 Hz) by Pacinian receptors. Sensitivity peaks around 250 Hz, decreasing above 320 Hz [2]. Based on these findings, PulseChord's operating range of 0–250 Hz targets the most perceptually salient frequencies, ensuring effective feedback while avoiding the diminishing sensitivity associated with higher frequencies. This range was confirmed through self-testing. It also aligns with standard audio engineering categories—covering sub-bass (20–60 Hz), bass (60–120 Hz), and upper bass/lower midrange (120–250 Hz)—allowing the system to deliver perceptually distinct and musically relevant tactile cues [3].

II. Applications

PulseChord is a versatile and low-cost haptic interface that translates live audio into meaningful tactile sensations. Its primary applications include enhancing music perception for deaf and hard of hearing individuals, allowing them to perceive rhythms, beats, and tonal structures through vibration, and providing immersive music experiences for hearing users. By filtering audio features into tactile frequency bands optimized for skin sensitivity, PulseChord offers an intuitive and non-visual representation of sound.

Beyond these core applications, PulseChord can process real-time environmental audio through its 3.5 mm input, delivering vibrotactile cues that enhance situational awareness for deaf and hard of hearing users and provide a more immediate sense of their surroundings. It also supports gaming and virtual reality by providing dynamic body-scale feedback synchronized with in-game events and environmental cues, enhancing spatial awareness and realism. Its analog design and minimal processing requirements make it well suited for wearable, low-latency applications where responsiveness and simplicity are critical.

III. Technical Overview

Stage	Description
Input	The audio input is split into three frequency bands. The first band (0–62.5 Hz) uses a third-order Sallen–Key low-pass filter, while the remaining bands (62.5–125 Hz and 125–250 Hz) are sixth-order band-pass networks formed by cascading third-order Sallen–Key high-pass and low-pass sections. This provides steep roll-off and minimal overlap, ensuring clear frequency separation.
Power	Each band passes through an inverting amplifier for impedance buffering and independent volume control. Filtered signals are then fed to individual Class D power amplifiers (TPA3110 XHA232, 30 W + 30 W stereo) powered by a LiPo supply. Two stereo amplifier modules are employed, utilizing three of the four available channels.
Output	The belt contains six speakers (4Ω, 5W each), two per frequency band: sub-bass at the center back, bass slightly outward, and upper bass at the outer edges. Each pair is wired in series (8Ω, 10W per band) and connected to a dedicated amplifier channel. These speakers are placed in close contact with the skin to maximize vibrational energy transfer.

Table 1: Overview of the three stages of PulseChord, summarizing the design and engineering of each stage.

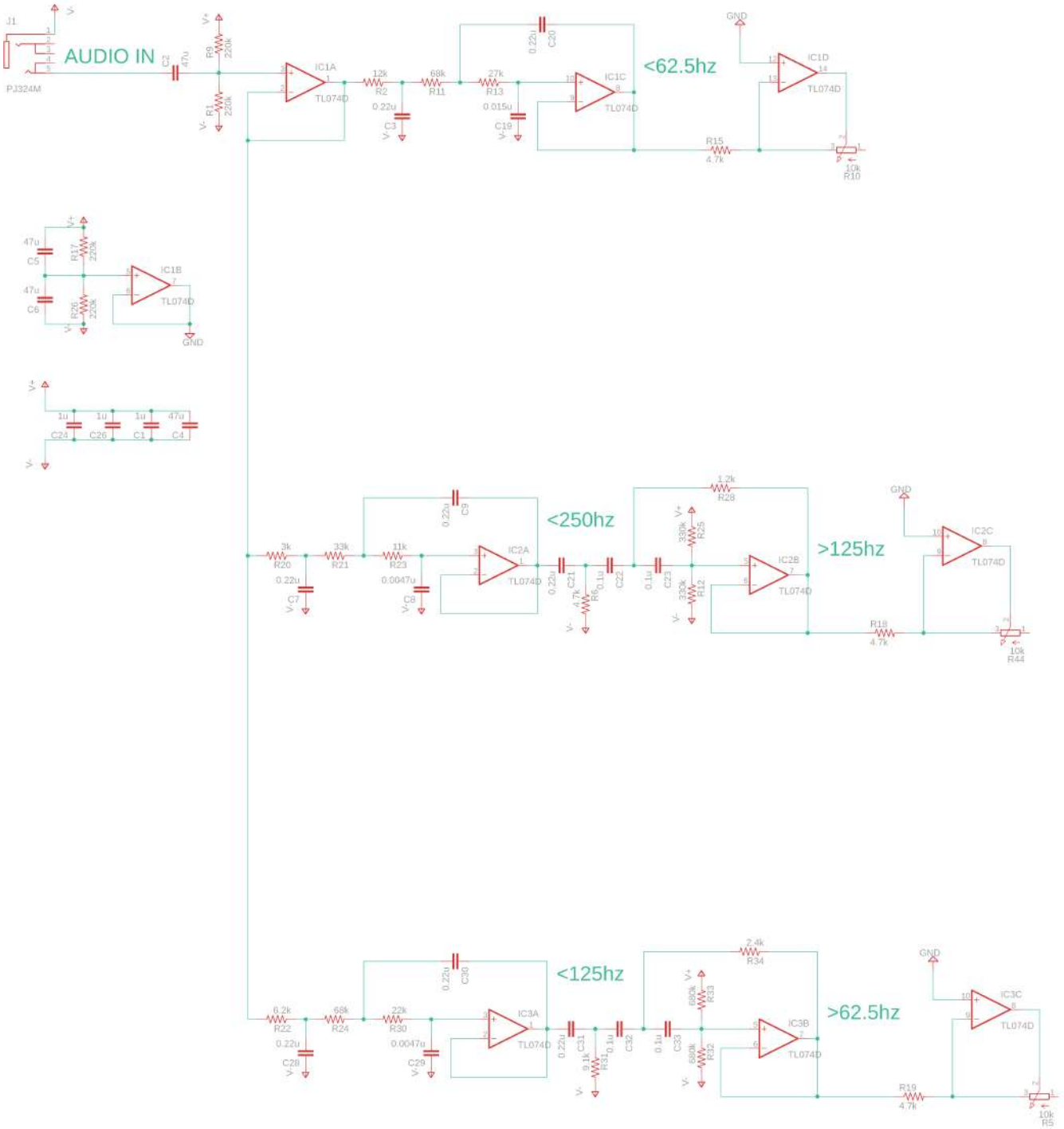

Figure 1: Full schematic, including biasing for unipolar supplies and standard, locally available components. Output capacitors are omitted, as the amplifier provides input coupling.

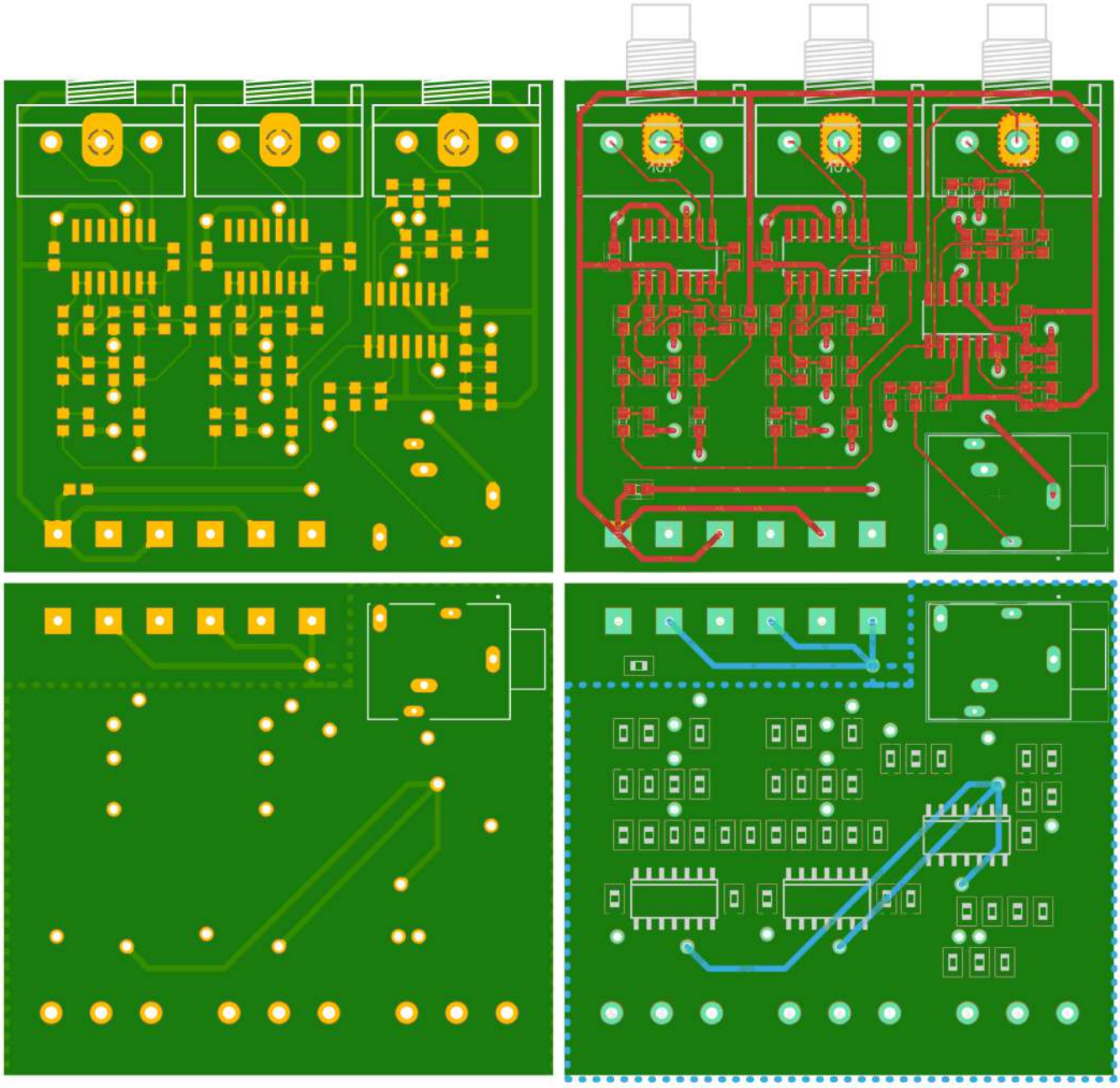

Figure 2: SMD, double-sided PCB with vias, designed to maximize electromagnetic compatibility (EMC) and ground loop protection within a compact, space-constrained layout.

Figure 3: Comparison of the FreeCAD 3D design of the speaker brace with the physical 3D-printed assembly and speaker.

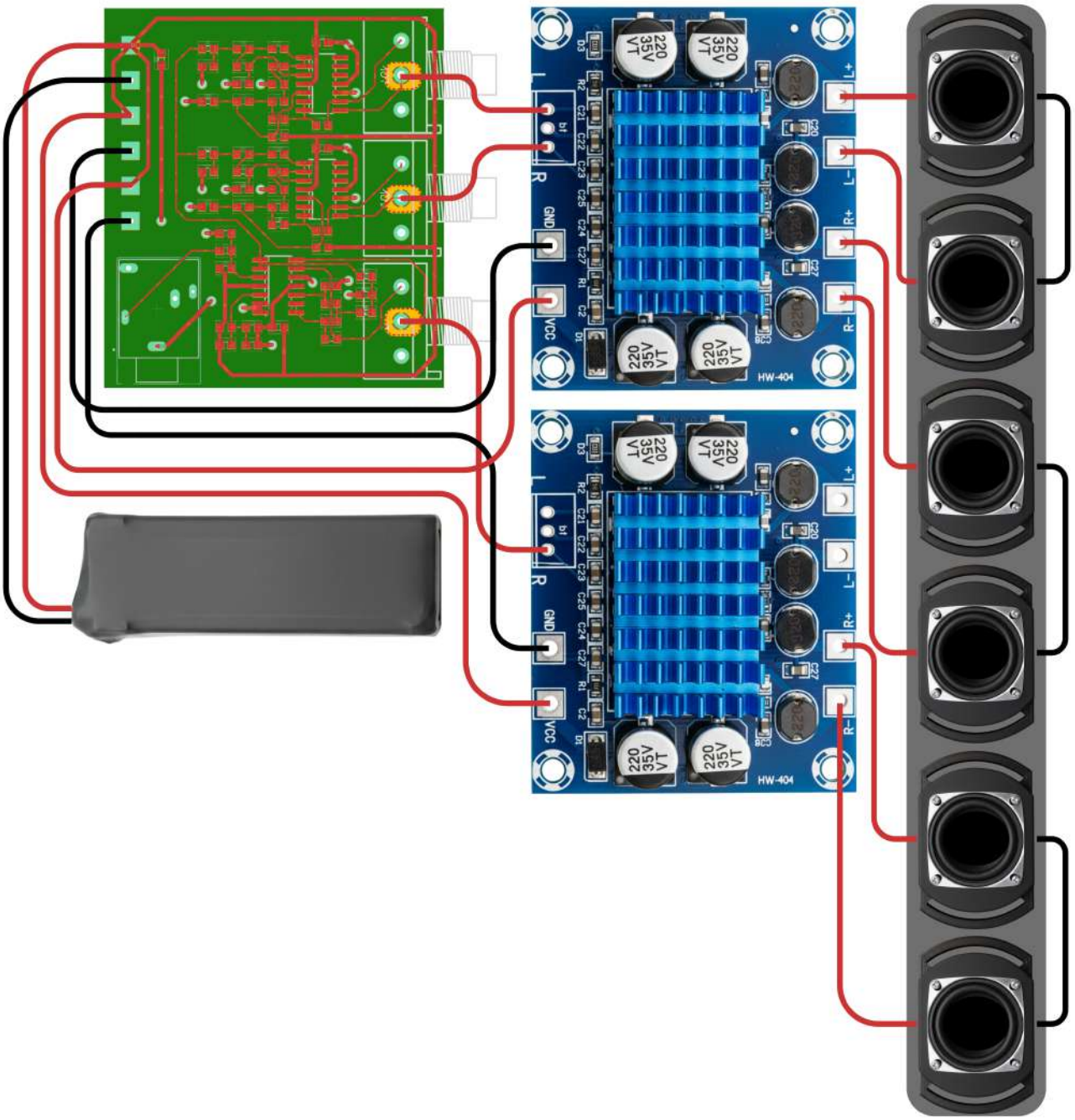

Figure 4: Visual circuit diagram of PulseChord, showing the band-separation circuit, amplifiers, battery, and speakers. Two amplifiers provide four channels, with one channel remaining unused.

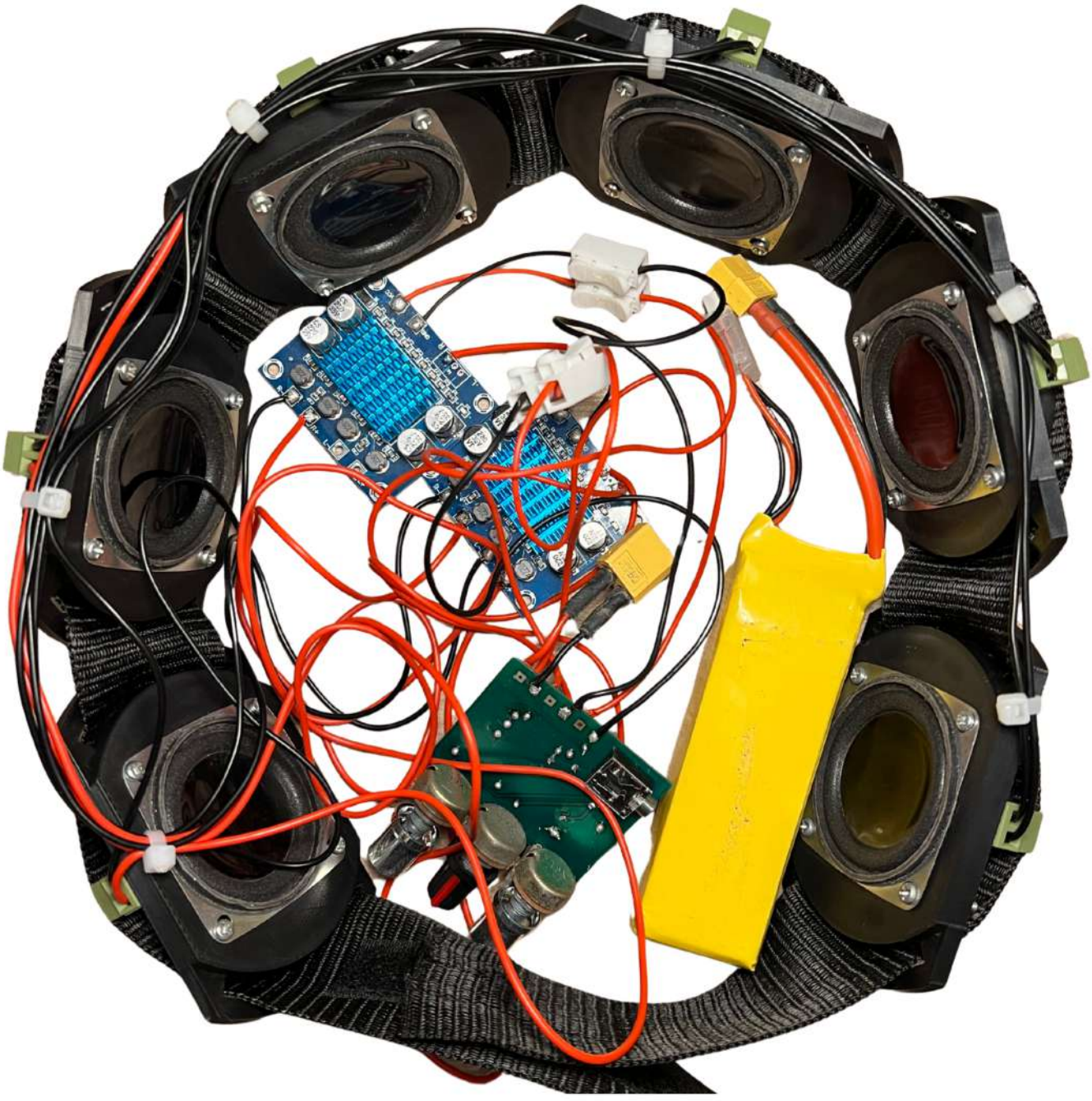

Figure 5: Speakers integrated into the thin nylon belt, approximately 3’4” in length with Velcro attachments, alongside the complete PulseChord system.

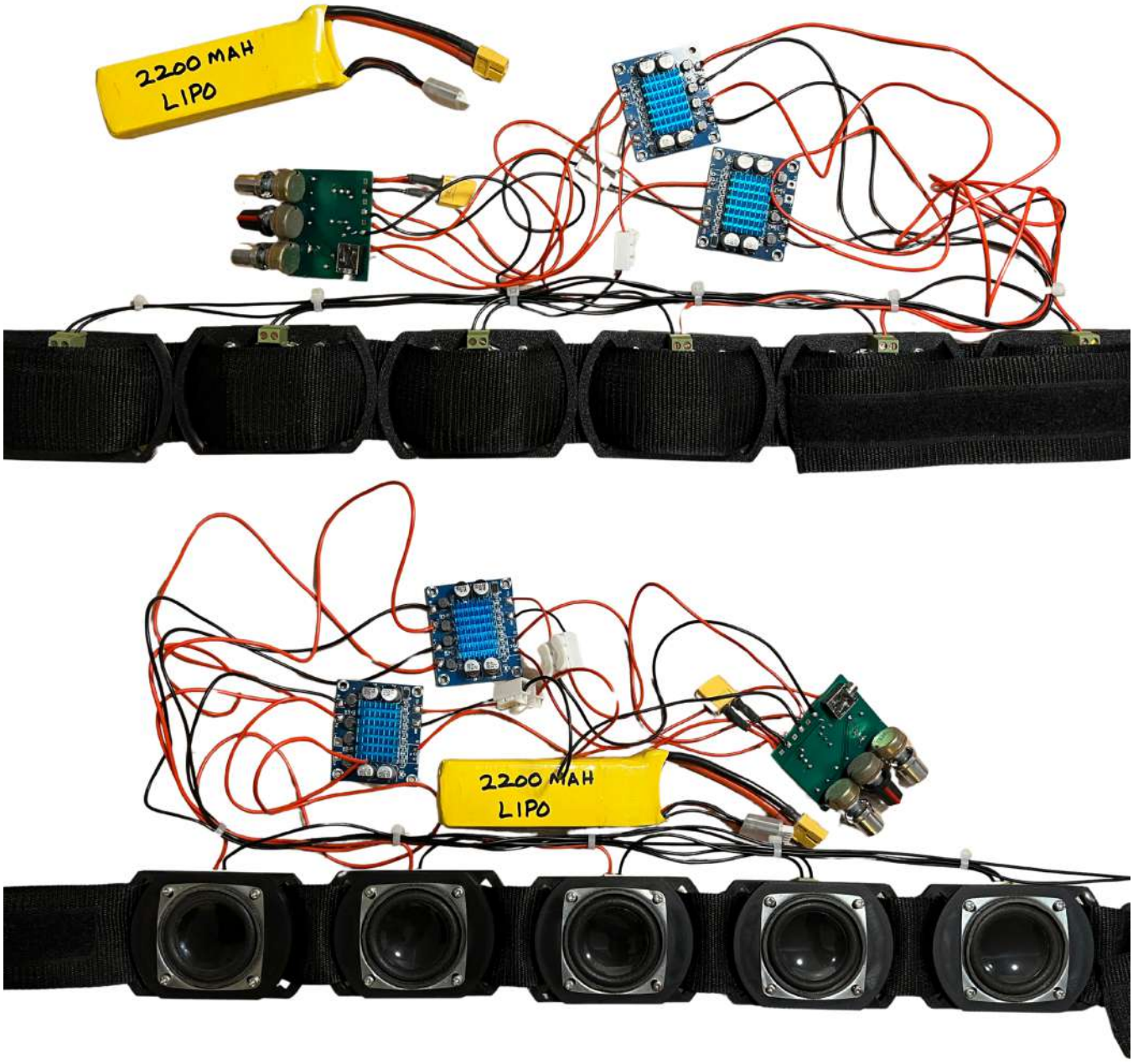

Figure 6: Front and back views of PulseChord alongside its internal circuitry.

Figure 7: PulseChord worn by the author.

Figure 8: Close-up view of PulseChord worn by the author.

IV. Modeling of Frequency Response

Modeling of both ideal and real frequency responses was performed using the available transfer functions [4].

$$H_{\mathrm{LP}}(s) = \frac{2\pi f_{c1}}{s+2\pi f_{c1}} \cdot \frac{(2\pi f_{c2})^2}{s^2+2\zeta(2\pi f_{c2})s+(2\pi f_{c2})^2} \tag{1}$$

$$H_{\mathrm{HP}}(s) = \frac{s}{s+2\pi f_{c1}} \cdot \frac{s^2}{s^2+2\zeta(2\pi f_{c2})s+(2\pi f_{c2})^2} \tag{2}$$

In an ideal configuration, f_{c1} and f_{c2} may be considered equivalent. These expressions can be combined into a full band-pass transfer function.

$$H_{\mathrm{BP}}(s) = H_{\mathrm{LP}}(s) \cdot H_{\mathrm{HP}}(s) \tag{3}$$

The 0–62.5 Hz frequency band operates exclusively as a low-pass region with the damping ratio $\zeta = 0.35$, while the band-pass regions each use $\zeta = 0.20$.

These values represent a compromise between achieving a steep roll-off near the cutoff frequencies and maintaining a flat response within the passband.

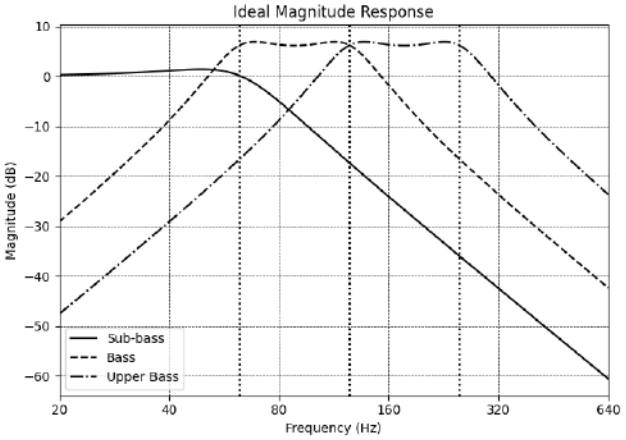

Figure 9: Magnitude response of the sub-bass, bass, and upper-bass filters.

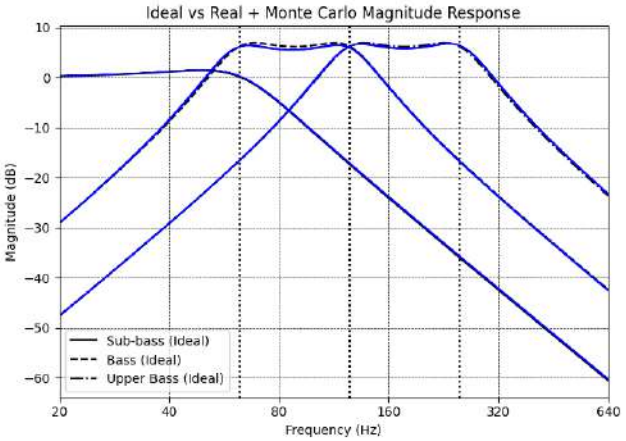

Figure 10: Monte Carlo simulation with ±1% resistor tolerance and ±0.25 pF capacitor tolerance, based on the actual E24 component values used. These value constraints introduce slight shifts in cutoff frequencies and damping ratio ζ.

V. Power Requirements

The calculation of power requirements begins by analyzing the input and simulating its propagation through the system to determine the total power consumption, including that of the output stage.

The average frequency distribution of songs was determined using the tool from [5] to extract data points from Fig 1 presented in [6]. This distribution represents the average of 772 songs over a time period of six decades.

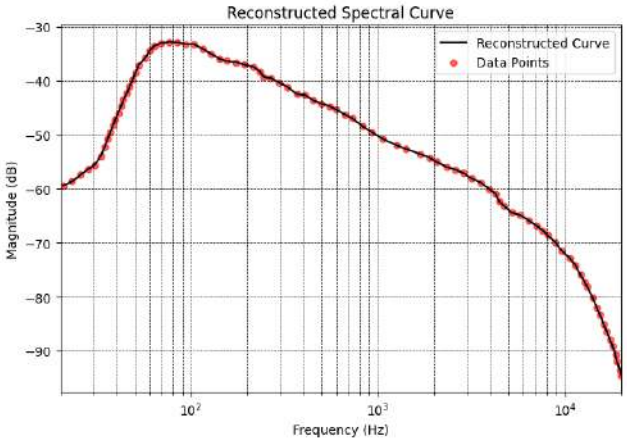

Figure 11: Close approximation of Fig 1 from [6].

These values must then be converted to a voltage scale, referenced to 1V peak-to-peak ($1/\sqrt{2}$V RMS). The domain should be converted from power to voltage, since the circuitry is based on op-amps.

Considering a peak output of 0.3V RMS from a conventional 3.5mm audio jack expected at the PulseChord input, the graph can be scaled to match this total voltage.

With a total voltage of $V_{\mathrm{total}} = \sqrt{\int V(f)^2 df} \approx 0.22$V RMS, a linear scaling factor of ≈ 1.4 is required. After scaling, the total voltage becomes $V_{\mathrm{RMS}} = \sqrt{\int V_{\mathrm{scaled}}(f)^2 df} \approx 0.3$V RMS.

This can then be used to calculate the total voltage of each individual band by passing the spectrum through the corresponding filter at maximum amplification and computing the resulting total.

The 20 dB amplification of the TPA3110 XH-A232, with GAIN0 and GAIN1 set to low, corresponds to a voltage gain of $\times 10$.

The individual speaker currents were calculated using Ohm's law for resistive loads:

$$I_k = \frac{V_k}{R_k}, \quad R_k = 8\ \Omega \tag{4}$$

The voltages and currents do not sum, as they exist in the AC domain; each amplifier operates independently in the AC domain, connected only through the parallel configuration in

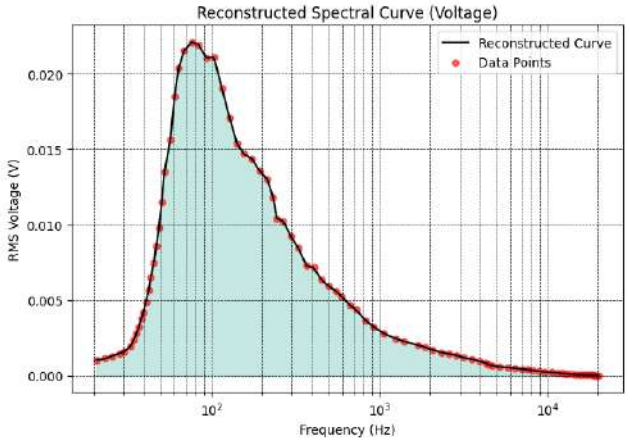

Figure 12: RMS voltage graph with corrected scaling to ensure a total voltage in accordance with the maximum total voltage of a 3.5mm audio jack.

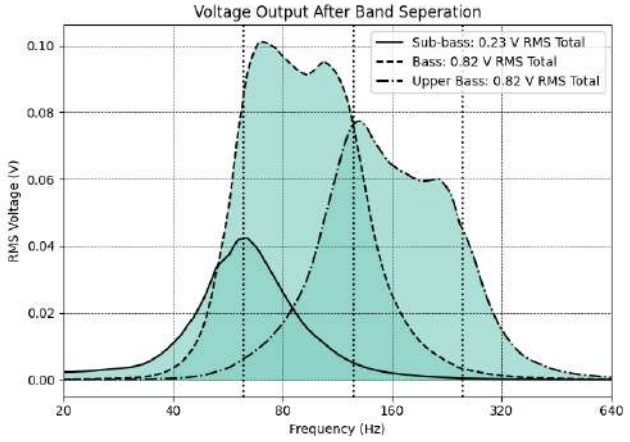

Figure 13: RMS voltage output after band separation. Inclusive of the maximum $\times 2.3$ amplification of the non-inverting output amplifiers

Metrics	Sub-bass	Bass	Upper Bass	Total
Before Amp	0.23V RMS	0.82V RMS	0.82V RMS	NA
After Amp	2.30V RMS	8.20V RMS	8.20V RMS	NA
Total Current	0.29A RMS	1.03A RMS	1.03A RMS	NA
Total Power	0.66W	8.40W	8.40W	17.5W
Power Drawn	0.73W	9.33W	9.33W	19.4W

Table 2: Final voltage, current, and power metrics for PulseChord at maximum operation, assuming 90% amplifier efficiency. Current drawn by the PulseChord circuitry is considered negligible due to the very low consumption of the TL074 op-amp.

the DC domain.

The total real power delivered to the speakers is the sum of the individual powers. Assuming purely resistive loads for simplicity (i.e., $\cos\phi_k \approx 1$), each speaker power is

$$P_k = V_k I_k \tag{5}$$

so the total power is

$$P_{\text{total}} = \sum_k P_k = \sum_k V_k I_k \tag{6}$$

The final power delivered by the amplifier was calculated by applying the 90% efficiency associated with the TPA3110 XHA232 to the total real power previously calculated.

Table 2 shows the average metrics calculated from the mean frequency spectrum of songs. Sub-bass power appears low because these frequencies occur less often, so averaging over time reduces their contribution. Instantaneous voltage, current, and power fluctuate, but over long periods they converge to the reported averages.

Since total real power is the only quantity conserved between the AC and DC domains, the battery current must be calculated from the total real power consumption.

$$I_{\text{battery}} = \frac{P_{\text{total}}}{V_{\text{battery}}} = \frac{19.4\text{W}}{11.1\text{V}} = 1.75\text{A} \tag{7}$$

The theoretical peak output voltage is

$$V_{\text{peak}} \approx 8.20\sqrt{2}\text{V} \approx 11.6\text{V} \tag{8}$$

Though the actual peak is expected to be lower due to the multi-frequency structure of typical audio signals. Accordingly, the calculations assume an 11.1V supply, as used in PulseChord, which remains sufficient given that 11.6V represents an extreme theoretical upper bound.

Based on this current draw, the 11.1V 2200mAh battery is expected to provide approximately 1 hour and 15 minutes of continuous operation for *musical* purposes at the theoretical maximum drive level.

VI. Stereo Support

The system can be upgraded to full stereo operation by adding a second set of band-separation filters for the additional audio channel. Since the belt already uses symmetrical left–right speaker pairs for each frequency band, only minimal changes to the hardware layout are required; each stereo channel would simply drive its own set of three filtered bands. The main trade-off is an increase in the number of components and the cost, but the overall architecture remains unchanged.

VII. Key Design Choices

Voice coil actuators were selected over standard ERM or LRA haptic motors to maintain low component costs

while enabling a broad, linear frequency response (20–250 Hz). This wide operating range is essential for the precise reproduction of complex musical textures, offering a level of fidelity and dynamic resolution that narrowband haptic alternatives cannot resolve.

Moreover, the power architecture balances mobility with endurance. While the integrated battery prioritizes untethered movement (e.g., performance, VR), the system also supports an external DC wall adapter. This enables continuous, long-duration operation, which is critical for providing sustained non-auditory access to music for the deaf or hard of hearing, as well as for other extended stationary usage scenarios like studio monitoring or seated gaming.

VIII. Future Work

Future work will focus on conducting subjective user studies with deaf and hard of hearing participants to validate perceptual effectiveness across a diverse demographic.

Acknowledgement

This work was conducted independently and received no external funding or sponsorship.

References

[1] EPCI, *The Science of Touch in Electronics: Haptics – It Used to Be All About Resonant Frequency*, EPCI, 2022. https://epci.eu/the-science-of-touch-in-electronics-haptics-it-used-to-be-all-about-resonant-frequency

[2] A. Ojala-Salo, *The Value of Tactile Sound in Music Perception*, Master's Thesis, Tampere University, 2023. https://trepo.tuni.fi/bitstream/handle/10024/148467/Ojala-SaloAnnukka.pdf;jsessionid=5B16A6F2D8008CA5DE7E0D88080B4750?sequence=2

[3] TeachMeAudio, *Understanding the Audio Spectrum*, n.d. https://www.teachmeaudio.com/mixing/techniques/audio-spectrum

[4] Okawa Denshi, *Sallen-Key Low-Pass Filter Design Tool*, n.d. http://sim.okawa-denshi.jp/en/Fkeisan.htm

[5] Automeris, *Automeris Online Tools*, n.d. https://automeris.io

[6] Pestana, Pedro, Ma, Zheng, Reiss, Joshua, Barbosa, Álvaro, & Black, Dawn, *Spectral characteristics of popular commercial recordings 1950–2010*, 2013. https://www.researchgate.net/publication/274511175_Spectral_characteristics_of_popular_commercial_recordings_1950-2010